

# Current Biology

## Animal-Borne Metrics Enable Acoustic Detection of Blue Whale Migration

### Highlights

- Acoustic monitoring reveals patterns in population-level blue whale song production
- Tag-derived metrics provide behavioral context for distinct diel patterns in song
- When integrated, tag and acoustic metrics reveal an acoustic signature of migration
- Key to discerning timing, plasticity, and drivers of a dispersed migration

### Authors

William K. Oestreich,  
James A. Fahlbusch, David E. Cade, ...,  
Brandon L. Southall,  
Jeremy A. Goldbogen, John P. Ryan

### Correspondence

woestreich@stanford.edu

### In Brief

Oestreich et al. integrate long-term acoustic monitoring and tag-derived metrics to identify an acoustic signature of blue whales' transition from foraging to migration. This finding links individual and population-level behavior in a highly dispersed population and is central to discerning timing, plasticity, and drivers of blue whale migration.

Report

# Animal-Borne Metrics Enable Acoustic Detection of Blue Whale Migration

William K. Oestreich,<sup>1,8,\*</sup> James A. Fahlbusch,<sup>1,2</sup> David E. Cade,<sup>1,3</sup> John Calambokidis,<sup>2</sup> Tetyana Margolina,<sup>4</sup> John Joseph,<sup>4</sup> Ari S. Friedlaender,<sup>3,5</sup> Megan F. McKenna,<sup>1</sup> Alison K. Stimpert,<sup>6</sup> Brandon L. Southall,<sup>3,5</sup> Jeremy A. Goldbogen,<sup>1</sup> and John P. Ryan<sup>7</sup>

<sup>1</sup>Hopkins Marine Station, Department of Biology, Stanford University, 120 Ocean View Blvd, Pacific Grove, CA 93950, USA

<sup>2</sup>Cascadia Research Collective, 218 1/2 W 4<sup>th</sup> Ave, Olympia, WA 98501, USA

<sup>3</sup>Institute of Marine Sciences, University of California Santa Cruz, 1156 High St, Santa Cruz, CA 95064, USA

<sup>4</sup>Naval Postgraduate School, 1 University Circle, Monterey, CA 93943, USA

<sup>5</sup>Southall Environmental Associates (SEA), Inc., 9099 Soquel Dr, Aptos, CA 95003, USA

<sup>6</sup>Moss Landing Marine Laboratories, 8272 Moss Landing Rd, Moss Landing, CA 95039, USA

<sup>7</sup>Monterey Bay Aquarium Research Institute, 7700 Sandholdt Rd, Moss Landing, CA 95039, USA

<sup>8</sup>Lead Contact

\*Correspondence: [woestreich@stanford.edu](mailto:woestreich@stanford.edu)

<https://doi.org/10.1016/j.cub.2020.08.105>

## SUMMARY

Linking individual and population scales is fundamental to many concepts in ecology [1], including migration [2, 3]. This behavior is a critical [4] yet increasingly threatened [5] part of the life history of diverse organisms. Research on migratory behavior is constrained by observational scale [2], limiting ecological understanding and precise management of migratory populations in expansive, inaccessible marine ecosystems [6]. This knowledge gap is magnified for dispersed oceanic predators such as endangered blue whales (*Balaenoptera musculus*). As capital breeders, blue whales migrate vast distances annually between foraging and breeding grounds, and their population fitness depends on synchrony of migration with phenology of prey populations [7, 8]. Despite previous studies of individual-level blue whale vocal behavior via bio-logging [9, 10] and population-level acoustic presence via passive acoustic monitoring [11], detection of the life history transition from foraging to migration remains challenging. Here, we integrate direct high-resolution measures of individual behavior and continuous broad-scale acoustic monitoring of regional song production (Figure 1A) to identify an acoustic signature of the transition from foraging to migration in the Northeast Pacific population. We find that foraging blue whales sing primarily at night, whereas migratory whales sing primarily during the day. The ability to acoustically detect population-level transitions in behavior provides a tool to more comprehensively study the life history, fitness, and plasticity of population behavior in a dispersed, capital breeding population. Real-time detection of this behavioral signal can also inform dynamic management efforts [12] to mitigate anthropogenic threats to this endangered population [13, 14].

## RESULTS

During the time of year when blue whales sing off central California, their song (Figure 1A) dominates the low-frequency soundscape (Figure 1B), making passive acoustic monitoring (PAM) a valuable tool for studying their ecology. However, PAM for the study of vocal populations is limited by (1) a scarcity of continuous, multiyear acoustic data streams; and (2) a lack of behavioral context for detected vocalizations via direct measurement of individual behavior over days to weeks, both of which are critical for the study of key life history transitions such as that from foraging to migration. Here, we integrate population and individual-level measurements, first analyzing 5 years of blue whale song from nearly continuous PAM data in the California Current Large Marine Ecosystem (CCLME) to quantify vocal behavior at the regional population level. We then use whale-borne tags ( $n = 15$  deployments) to measure the vocal, foraging, and migratory

behavior of individuals simultaneously in the same ecosystem. These direct measures of behavior allow us to decipher the individual-level context of population-level patterns in vocal behavior and uncover an acoustically detectable transition from foraging to migration in blue whales at the regional population level.

### Population-Level Vocal Behavior

We analyzed acoustic data collected from a hydrophone in the central CCLME [15] (Figure 1B) to quantify population-level vocal behavior. This instrument samples a large area (Figure 2A) of blue whale foraging habitat [16, 17] in and around Monterey Bay, California. By “population-level,” we mean that we characterized vocally active individuals (singing males) collectively, in the context of population-level migration. Two linked metrics of blue whale song production were used to quantify regional population-level vocal behavior (see STAR Methods for details): “call

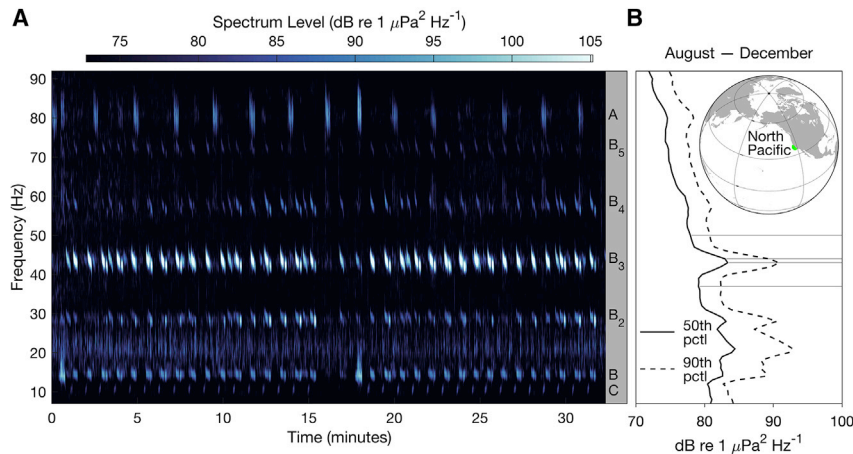


**Figure 1. Blue Whale Song in the Low-Frequency Soundscape of Coastal California**

(A) Example of blue whale song, comprised of patterned sequences of A, B, and C calls; for B calls, fundamental (B) and harmonic (B<sub>2-5</sub>) frequencies are labeled. This song was recorded through the Monterey Accelerated Research System (MARS) cabled observatory (green circle in inset map in graphic B) (36.713°N, 122.186°W, 891 m depth). (B) 50<sup>th</sup> and 90<sup>th</sup> percentile of MARS daily mean spectrum levels during August–December, 2015–2019, when blue whale song is prevalent. Gray lines indicate the frequencies used to compute CI of the B call third harmonic (see STAR Methods for details). Both graphs share a single y axis. See also Figure S1.

index” (CI) (a metric of blue whale song intensity) and  $CI_{\text{night}}:CI_{\text{day}}$ , the ratio of blue whale song intensity during night versus day. Like the majority of acoustic research on this population, CI focuses on the song-associated B call (Figure 1), because of its predictable spectral characteristics, its detectability over vast distances (hundreds of km [18]) (Figure 2A), and its status as the most common and highest amplitude unit of the song-associated vocalizations [19]. Although thought to be produced exclusively by males, we assume song production in relation to migration to be representative of population-level migratory behavior in both sexes because of evidence of population-wide seasonal synchrony in departure from higher-latitude foraging grounds [20] and observations of increased male-female pair associations immediately preceding migration [21].

Monthly aggregated distributions of daily CI and  $CI_{\text{night}}:CI_{\text{day}}$  show distinct seasonal and diel patterns (Figure 2). The annual cycle of CI shows a rise in song during summer-fall, peaking in November (Figure 2B). This peak is followed by a steep decline in December-January before dropping to ~1 (little-to-no detectable song signal) for February-June. The annual cycle of  $CI_{\text{night}}:CI_{\text{day}}$  reveals a seasonal modulation of diel patterns in song production (Figure 2C). During the months of most rapid increase in

CI (August-September), median  $CI_{\text{night}}:CI_{\text{day}}$  rises from 1.16 (August) to 1.25 (September). Near the peak in CI (October-November), median  $CI_{\text{night}}:CI_{\text{day}}$  falls to 1.07. During the winter decline in CI (December-January), median  $CI_{\text{night}}:CI_{\text{day}}$  falls below 1, indicating greater song production during the day.

#### Individual-Level Feeding, Vocal, and Migratory Behavior

We analyzed 15 tag deployments totaling 664.13 h spread across 3 years (Figures 3A–3C): 2 medium-duration (32.1 and 18.3 day) deployments and 13 short-duration ( $0.8 \pm 0.5$  [mean  $\pm$  st. dev.] day) deployments. Tag data captured foraging, calling, and migratory behavior to provide individual-level behavioral context for population-level patterns in song production. We detected 3,968 song-associated A and B calls and 4,892 feeding lunges across these deployments (Table S1). Individual blue whales in a foraging behavioral state ( $n = 15$ ) displayed clear diel patterns in calling and feeding lunge behaviors, feeding during daylight hours and calling on shallow non-feeding dives during nights (Figure 3D). These individuals produced song-associated calls at rates of 9.2, 10.7, and 7.0 calls per h during nights in 2017, 2018, and 2019, respectively (Figure 3E). During daytime, song call rates were lower, at 2.9, 2.4, and 2.9 calls per h

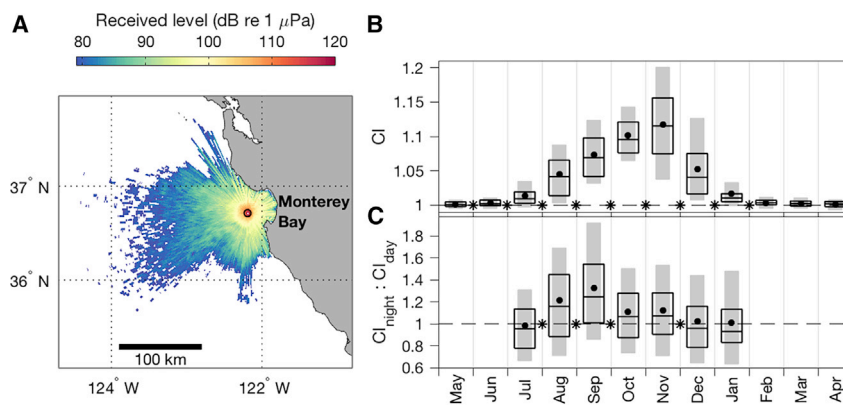


**Figure 2. Population-Level Vocal Behavior of Blue Whales**

(A) Modeled received level at the MARS (black circle) cabled observatory hydrophone, characterizing the detection range for B calls. Model results are shown for a sound source with frequency (44 Hz), depth (14.8 m, mean value of B call production from tag data in this study), and source level (171 dB re  $1\mu\text{Pa-m}$  [22]) representative of the third harmonic of blue whale B calls. Sound sources from areas with received level  $> 78$  dB re  $1\mu\text{Pa}$  are likely to be detected over median levels of ambient noise (Figure S1), indicating detection ranges  $> 100$  km. (B) Monthly binned statistics over 5 years (2015–2019) of blue whale B CI. Black boxes indicate 25<sup>th</sup>, 50<sup>th</sup>, and 75<sup>th</sup> percentiles of daily CI values from each month. Black dots indicate means. Gray bars indicate 10<sup>th</sup>–90<sup>th</sup> percentiles.

(C) Monthly binned statistics of  $CI_{\text{night}}:CI_{\text{day}}$ . Values  $> 1$  indicate greater nighttime song intensity; values  $< 1$  indicate greater daytime song intensity. For (B) and (C), asterisks indicate statistically significant ( $p < 0.05$ ) month-to-month changes in the mean. See also Figure S1.

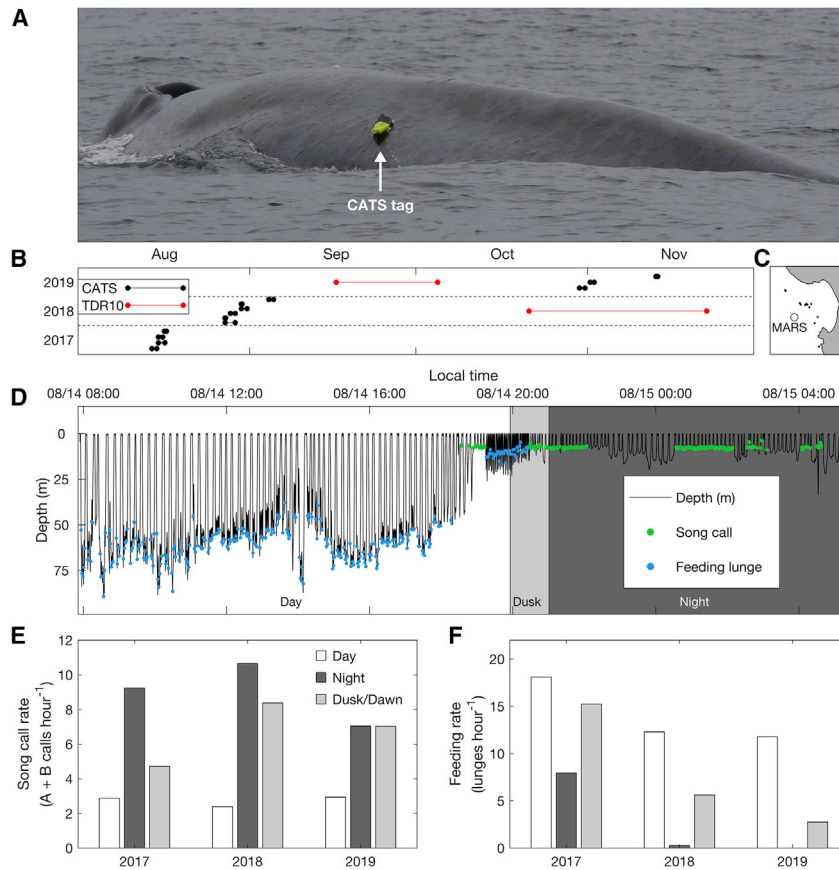


**Figure 3. Individual-Level Feeding and Vocal Behavior of Foraging Blue Whales (n = 15 Deployments; 664.13 h)**

(A) CATS tag deployed on a blue whale in Monterey Bay, CA. Photo taken under NMFS Permit #16111. (B) Temporal coverage of short-duration (CATS) and medium-duration (TDR10) tag deployments. (C) Deployment locations of CATS tags (black points) in relation to the MARS hydrophone.

(D) Representative example CATS tag deployment showing daytime feeding at depth, crepuscular near-surface feeding, and nighttime song production.

(E and F) In (E) are song call rates and in (F) are feeding lunge rates during foraging across all tag deployments 2017–2019 binned by solar elevation categories (night <  $-12^\circ$ ; dusk/dawn  $-12^\circ$  to  $0^\circ$ ; day >  $0^\circ$ ).

See also [Table S1](#).

during night ( $4.1 \pm 1.2$  calls per h) than it did during the day ( $1.3 \pm 0.6$  calls per h). This pattern inverted after the transition to southward migration, with night and day song call rates of  $3.1 \pm 0.5$  and  $9.6 \pm 1.7$  song calls per h, respectively. The mean of night-minus-day call rate (Figure 4B) before and after this transition were significantly different ( $p = 9.2e-05$ ). For both individuals, the patterns of song production observed after transition to migration were opposite those during

(Figure 3E). Feeding lunges showed an opposite diel pattern, with daytime lunge rates of 18.1, 12.2, and 11.8 lunges per h and nighttime lunge rates of 8.0, 0.3, and 0 in 2017, 2018, and 2019, respectively (Figure 3F). The individual-level patterns in song production observed during foraging (Figure 3E) matched those observed at the population level during the period from August–November (Figure 2C).

A behavioral state transition marked by cessation of foraging and transition to southward migration was detected by both medium-duration tag deployments on foraging individuals (Figure 4). One individual, who fed for the first  $\sim 10$  days of the deployment, recorded no feeding lunges for the final  $\sim 21$  days that coincided with southward movement  $>1,000$  km from a latitude of  $\sim 38$  to  $\sim 28^\circ$  N (Figure 4A). Before this behavioral state transition, this individual sang more frequently during night ( $13.0 \pm 1.6$  [daily mean  $\pm$  daily st. err.] song calls per h) than during day ( $3.2 \pm 1.0$  song calls per h). This pattern inverted after the transition: night and day song call rates were  $5.1 \pm 1.0$  and  $10.0 \pm 1.7$  song calls per h, respectively. The mean of daily values for night-minus-day call rate (Figure 4A) before and after this transition showed a statistically significant difference ( $p = 1.8e-06$ ). Another deployment on a different individual captured a similar behavioral transition from foraging to southward transit, again marked by an inverted diel pattern of song production after transition to southward migration (Figure 4B). During the first  $\sim 7$  days of this deployment, this individual foraged primarily during the day and also produced song calls more frequently

foraging, matching population-level patterns observed during December–January (Figure 2C).

## DISCUSSION

### Acoustic Signature of Migration

The difference in diel patterns of song production between foraging and migrating individual blue whales (Figures 3 and 4), plus the population-level inversion of this diel pattern preceding the cessation of acoustic detection (Figure 2), indicates a previously unrecognized acoustic signature of the population-level behavioral transition from foraging to southward migration. Using high-resolution individual-level behavioral data, we demonstrate that the strong diel patterning in vocal behavior during late summer and early fall is driven by a separation between foraging and singing behaviors (Figure 3). However, the favoring of nighttime song production lessens as individuals reduce daytime foraging effort in their transition to southward migration (Figure 4) toward lower-latitude breeding grounds typically occupied in winter and spring [20, 23, 24]. At the population level, the cumulative transition of individuals to this migratory and associated vocal behavior results in a reduction and eventual inversion of diel patterning in song production (Figure 2C). Although individual-level tag data collectively reveal the basis for greater song activity at night during summer and fall (Figure 2C) driven by daytime foraging behavior (Figure 3), two exceptional tag deployments reveal the basis for transition

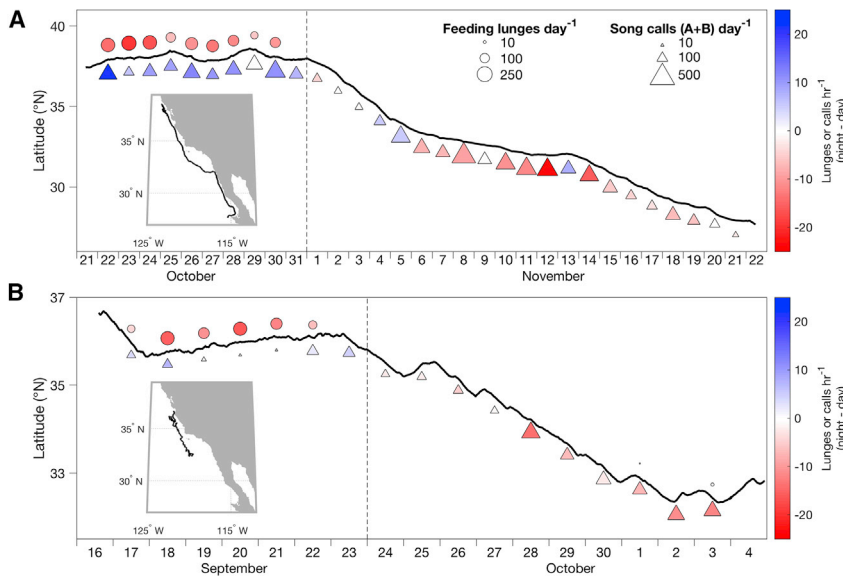


**Figure 4. Individual-Level Feeding and Vocal Behavior during Transition to Migration**

(A and B) Shown are (A) 2018 deployment and (B) 2019 deployment. On both graphics, the black line indicates animal latitude from its track (inset map). Circles above latitude line indicate daily feeding rate; triangles below indicate daily song call production rate. All daily feeding and song production rates colored by daytime (red) or nighttime (blue) tendency. See also [Table S1](#).

to greater song activity during day, driven by migratory behavior ([Figure 4](#)).

### Blue Whale Ecology and Conservation

This acoustic signature of the population-level transition from foraging to migration provides a significant advance in PAM: the translation of raw acoustic data to population ethograms. Such behavioral information has direct applications to understanding of blue whale ecology and effective management of this endangered species. Blue whales in the Northeast Pacific rely on energy stores built up during a summer-fall foraging season to fuel both migration to winter-spring lower-latitude breeding grounds and successful reproduction [7]. This migratory, foraging, and reproductive strategy, known as capital breeding [25], is tightly linked to the seasonal phenology of upwelling, primary productivity, and subsequent blooms of krill in the CCLME [8, 16]. In an ecosystem displaying variability on timescales ranging from hourly-to-daily (diurnal fluctuations in upwelling intensity [26]), weekly-to-seasonal (episodic and annual upwelling variation [27]), interannual (phenology and accumulation of upwelling productivity [28]), multi-annual/decadal (climate oscillations [29]), and longer-term (climate change [30]) scales, the cues that blue whales use to optimize this foraging and migratory strategy are not fully understood.

Recent work on northward migration in this population suggests a role of spatial memory and lack of behavioral plasticity to adapt to the changing distribution of biologically productive habitats in the CCLME [8]. Acoustics-only approaches, using local cessation of acoustic detection as a proxy for timing of migration, have suggested some temporal flexibility in migration [11]. Here, however, we show that individuals might begin migration 2–4 months before local cessation of population-level song detection ([Figure 2](#)), further emphasizing the importance of individual-level context in PAM. The acoustic signature of transition to migration identified here allows for more precise investigation into the timing, drivers, and plasticity of southward migration, an important consideration for understanding how blue whales will

respond to climate-driven changes in resource availability [30]. Furthermore, timing of the population-level transition to southward migration might act as an acoustic ecosystem indicator [31], providing near-real-time information about forage availability over the vast distances at which blue whale song can be detected.

This acoustic signature of blue whale behavior might also provide near-real-

time information necessary for dynamic management strategies [12]. Detection of population behavior from acoustics alone can inform efforts to reduce ship strikes, a human-wildlife conflict issue in areas of high ship and whale overlap [13]. Advance notice on the timing of southward migration from key foraging areas (e.g., Monterey Bay) might inform prediction of when migrating blue whales will encounter relatively high vessel-strike risk in areas such as the Santa Barbara Channel [13], or anthropogenic noise disturbance [14], toward reducing threats to this endangered and once near-extinct population [32].

### Linking Individual- and Population-Level Migration

Understanding how behavior at the individual level manifests in population-level movements is central to explaining the mechanisms and cues of collective behaviors such as migration [2, 3]. These linkages between individual and population behavior have long challenged scientists, and emerging techniques (e.g., bioacoustics [33] and bio-logging [34, 35]) have been proposed as tools to advance understanding in both marine and terrestrial ecosystems. The ability to observe individual animals' behaviors with increasing detail has revolutionized behavioral ecology [34, 35], yet extrapolation to population behavior largely relies on statistical modeling techniques. Over the last half-century, PAM has been widely employed to study behavior at the population level, yet interpretation is limited by sparse individual-level behavioral context [10, 33, 36]. Similarly, other population-level approaches to studying migratory behavior (e.g., radar for observing bird [37, 38] and insect [39] migrations) often lack—but can be enhanced by—integration with direct measures of individual-level behavior. Here, we present a unique empirical approach to integrating technologies and levels of observation to address questions of behavioral ecology that require linking individual and population-level behavior.

For example, collective migration is observable at the population level and results from individual behavioral decisions incorporating personal and/or social information [3, 40]. This has been explored in depth for groups of proximate migratory individuals

[2, 3, 41]. This blue whale study holds promise for expanding our understanding of the relative roles of individual sensory information and social interactions in migration at a scale that has been difficult to observe, and in a highly dispersed population that would require long-distance communication rather than proximate social cues for coordinated (intentional or unintentional) collective behavior. Synchrony of the population-level transition in diel vocal behavior with the peak in overall song production (Figure 2) and subsequent southward migration suggests a role of song in collective southward migration. In an enormous potential foraging area comprised of diverse and dynamic oceanographic habitat, no individual blue whale can assess regional foraging conditions to make an “informed” decision about transitioning from foraging to southward migration. Diel song patterns (and associated behavior) from distant conspecifics might provide social information about broader forage availability and ultimately influence individual decision making. Previous work suggests that compared with dense groups of organisms, dispersed populations should struggle to collectively sense and appropriately respond to environmental information [42]. Yet the ability to communicate over vast distances could invert this paradigm and make dispersion beneficial. The patchiness and ephemerality of blue whale prey resources [43], the extreme physiology and metabolic demands of blue whales [44], and their evolution of long-distance vocalizations are all suggestive of acoustic social cues that might contribute to population fitness. Although further investigation into the potential roles of individual sensory information and long-distance social cues through song is necessary to fully understand the drivers of southward migration in this population, the ability to acoustically detect this population-level behavioral transition improves our capacity to understand blue whale behavior and, more broadly, collective migration.

## STAR★METHODS

Detailed methods are provided in the online version of this paper and include the following:

- **KEY RESOURCES TABLE**
- **RESOURCE AVAILABILITY**
  - Lead Contact
  - Materials Availability
  - Data and Code Availability
- **EXPERIMENTAL MODEL AND SUBJECT DETAILS**
- **METHOD DETAILS**
  - Population-level behavior
  - Individual-level behavior
- **QUANTIFICATION AND STATISTICAL ANALYSIS**

## SUPPLEMENTAL INFORMATION

Supplemental Information can be found online at <https://doi.org/10.1016/j.cub.2020.08.105>.

## ACKNOWLEDGMENTS

W.K.O. is supported by the National Science Foundation Graduate Research Fellowship Program (NSFGRFP) and as a David and Lucile Packard Foundation Stanford Graduate Fellow. The NSF funded installation and maintenance

of the MARS cabled observatory through awards 0739828 and 1114794. Hydrophone recording through MARS was supported by the Monterey Bay Aquarium Research Institute, through a grant from the David and Lucile Packard Foundation. Thanks to C. Dawe, D. French, K. Heller, P. McGill, and the crew of the R/V Rachel Carson for design, deployment, and maintenance of the MARS hydrophone hardware system and to D. Cline and P. McGill for the decimated PAM data used in this study. Tagging efforts were funded by National Science Foundation Integrative Organismal Systems (NSF IOS) grant 1656691, Office of Naval Research (ONR) grants N00014-13-1-0772 and N00014-14-1-0414, and Office of Naval Research/Living Marine Resources (ONR/LMR) grants N39430-16-C-1853 and N39430-15-C-1692. Additional funding for 2019 field efforts was provided by the California Ocean Alliance. Thank you to the crew of the R/V John Martin for support in the 2017 and 2018 tagging efforts. Thank you also to M. Chapman, M. Savoca, and three anonymous reviewers for comments that improved this manuscript.

## AUTHOR CONTRIBUTIONS

Conceptualization, W.K.O., J.A.G., and J.P.R.; Methodology, W.K.O., J.A.F., D.E.C., J.C., A.S.F., J.A.G., and J.P.R.; Formal Analysis, W.K.O., J.A.F., D.E.C., T.M., J.J., and J.P.R.; Visualization, W.K.O. and J.P.R.; Writing – Original Draft, W.K.O.; Writing – Reviewing and Editing, all authors.

## DECLARATION OF INTERESTS

The authors declare no competing interests.

Received: June 8, 2020

Revised: July 31, 2020

Accepted: August 31, 2020

Published: October 1, 2020

## REFERENCES

1. Levin, S.A. (1992). The problem of pattern and scale in ecology. *Ecology* 73, 1943–1967.
2. Torney, C.J., Hopcraft, J.G.C., Morrison, T.A., Couzin, I.D., and Levin, S.A. (2018). From single steps to mass migration: the problem of scale in the movement ecology of the Serengeti wildebeest. *Philos. Trans. R. Soc. Lond. B Biol. Sci.* 373, 20170012.
3. Couzin, I.D. (2018). Collective animal migration. *Curr. Biol.* 28, R976–R980.
4. Alerstam, T., Hedenström, A., and Åkesson, S. (2003). Long-distance migration: Evolution and determinants. *Oikos* 103, 247–260.
5. Tucker, M.A., Böhning-Gaese, K., Fagan, W.F., Fryxell, J.M., Van Moorter, B., Alberts, S.C., Ali, A.H., Allen, A.M., Attias, N., Avgar, T., et al. (2018). Moving in the Anthropocene: Global reductions in terrestrial mammalian movements. *Science* 359, 466–469.
6. Hays, G.C., Ferreira, L.C., Sequeira, A.M.M., Meekan, M.G., Duarte, C.M., Bailey, H., Baillieu, F., Bowen, W.D., Caley, M.J., Costa, D.P., et al. (2016). Key Questions in Marine Megafauna Movement Ecology. *Trends Ecol. Evol.* 31, 463–475.
7. Pirota, E., Mangel, M., Costa, D.P., Mate, B., Goldbogen, J.A., Palacios, D.M., Hückstädt, L.A., McHuron, E.A., Schwarz, L., and New, L. (2018). A dynamic state model of migratory behavior and physiology to assess the consequences of environmental variation and anthropogenic disturbance on marine vertebrates. *Am. Nat.* 191, E40–E56.
8. Abrahms, B., Hazen, E.L., Aikens, E.O., Savoca, M.S., Goldbogen, J.A., Bograd, S.J., Jacox, M.G., Irvine, L.M., Palacios, D.M., and Mate, B.R. (2019). Memory and resource tracking drive blue whale migrations. *Proc. Natl. Acad. Sci. USA* 116, 5582–5587.
9. Lewis, L.A., Calambokidis, J., Stimpert, A.K., Fahlbusch, J., Friedlaender, A.S., McKenna, M.F., Mesnick, S.L., Oleson, E.M., Southall, B.L., Szesciorka, A.R., and Širović, A. (2018). Context-dependent variability in blue whale acoustic behaviour. *R. Soc. Open Sci.* 5, 180241.

10. Oleson, E.M., Calambokidis, J., Burgess, W.C., McDonald, M.A., LeDuc, C.A., and Hildebrand, J.A. (2007). Behavioral context of call production by eastern North Pacific blue whales. *Mar. Ecol. Prog. Ser.* 330, 269–284.
11. Szesciorka, A.R., Ballance, L.T., Širović, A., Rice, A., Ohman, M.D., Hildebrand, J.A., and Franks, P.J.S. (2020). Timing is everything: Drivers of interannual variability in blue whale migration. *Sci. Rep.* 10, 7710.
12. Oestreich, W.K., Chapman, M.S., and Crowder, L.B. A comparative analysis of dynamic management in marine and terrestrial systems. *Front. Ecol. Environ.* 10.1002/fee.2243.
13. Redfern, J.V., McKenna, M.F., Moore, T.J., Calambokidis, J., Deangelis, M.L., Becker, E.A., Barlow, J., Forney, K.A., Fiedler, P.C., and Chivers, S.J. (2013). Assessing the risk of ships striking large whales in marine spatial planning. *Conserv. Biol.* 27, 292–302.
14. Goldbogen, J.A., Southall, B.L., DeRuiter, S.L., Calambokidis, J., Friedlaender, A.S., Hazen, E.L., Falcone, E.A., Schorr, G.S., Douglas, A., Moretti, D.J., et al. (2013). Blue whales respond to simulated mid-frequency military sonar. *Proc. Biol. Sci.* 280, 20130657.
15. Ryan, J., Cline, D., Dawe, C., McGill, P., Zhang, Y., Joseph, J., Margolina, T., Caillat, M., Fischer, M., Devogelaere, A., et al. (2016). New Passive Acoustic Monitoring in Monterey Bay National Marine Sanctuary. OCEANS 2016 MTS/IEEE Monterey, CA, 1–8.
16. Croll, D.A., Marinovic, B., Benson, S., Chavez, F.P., Black, N., Ternullo, R., and Tershy, B.R. (2005). From wind to whales: Trophic links in a coastal upwelling system. *Mar. Ecol. Prog. Ser.* 289, 117–130.
17. Calambokidis, J., Steiger, G.H., Curtice, C., Harrison, J., Ferguson, M.C., Becker, E., DeAngelis, M., and Van Parijs, S.M. (2015). Biologically important areas for selected cetaceans within U.S. waters - West Coast region. *Aquat. Mamm.* 41, 39.
18. Stafford, K.M., Fox, C.G., and Clark, D.S. (1998). Long-range acoustic detection and localization of blue whale calls in the northeast Pacific Ocean. *J. Acoust. Soc. Am.* 104, 3616–3625.
19. Širović, A., Rice, A., Chou, E., Hildebrand, J.A., Wiggins, S.M., and Roch, M.A. (2015). Seven years of blue and fin whale call abundance in the Southern California Bight. *Endanger. Species Res.* 28, 61–76.
20. Bailey, H., Mate, B.R., Palacios, D.M., Irvine, L., Bograd, S.J., and Costa, D.P. (2010). Behavioural estimation of blue whale movements in the Northeast Pacific from state-space model analysis of satellite tracks. *Endanger. Species Res.* 10, 93–106.
21. Sears, R., and Perrin, W.F. (2009). Blue whale: *Balaenoptera musculus*. In *Encyclopedia of Marine Mammals*, W.F. Perrin, B. Würsig, and J.G.M. Thewissen, eds. (Academic Press), pp. 120–124.
22. Thode, A.M., D’Spain, G.L., and Kuperman, W.A. (2000). Matched-field processing, geoacoustic inversion, and source signature recovery of blue whale vocalizations. *J. Acoust. Soc. Am.* 107, 1286–1300.
23. Stafford, K.M., Nieuwkirk, S.L., and Fox, C.G. (1999). An acoustic link between blue whales in the eastern tropical Pacific and the Northeast Pacific. *Mar. Mamm. Sci.* 15, 1258–1268.
24. Stafford, K., Nieuwkirk, S., and Fox, C. (2001). Geographic and seasonal variation of blue whale calls in the North Pacific. *J. Cetacean Res. Manag.* 3, 65–76.
25. Jönsson, K.I. (1997). Capital and Income Breeding as Alternative Tactics of Resource Use in Reproduction. *Oikos* 78, 57–66.
26. Woodson, C.B., Eerkes-Medrano, D.I., Flores-Morales, A., Foley, M.M., Henkel, S.K., Hessing-Lewis, M., Jacinto, D., Needles, L., Nishizaki, M.T., O’Leary, J., et al. (2007). Local diurnal upwelling driven by sea breezes in northern Monterey Bay. *Cont. Shelf Res.* 27, 2289–2302.
27. Benoit-Bird, K.J., Waluk, C.M., and Ryan, J.P. (2019). Forage Species Swarm in Response to Coastal Upwelling. *Geophys. Res. Lett.* 46, 1537–1546.
28. Henson, S.A., and Thomas, A.C. (2007). Interannual variability in timing of bloom initiation in the California Current System. *J. Geophys. Res. Ocean.* 112, <https://doi.org/10.1029/2006JC003960>.
29. Chavez, F.P., Ryan, J., Lluch-Cota, S.E., and Niquen, C. M. (2003). From anchovies to sardines and back: multidecadal change in the Pacific Ocean. *Science* 299, 217–221.
30. Roemmich, D., and McGowan, J. (1995). Climatic warming and the decline of zooplankton in the California current. *Science* 267, 1324–1326.
31. Hazen, E.L., Abrahms, B., Brodie, S., Carroll, G., Jacox, M.G., Savoca, M.S., Scales, K.L., Sydeman, W.J., and Bograd, S.J. (2019). Marine top predators as climate and ecosystem sentinels. *Front. Ecol. Environ.* 17, 565–574.
32. Thomas, P.O., Reeves, R.R., and Brownell, R.L. (2016). Status of the world’s baleen whales. *Mar. Mamm. Sci.* 32, 682–734.
33. Blumstein, D.T., Mennill, D.J., Clemins, P., Girod, L., Yao, K., Patricelli, G., Deppe, J.L., Krakauer, A.H., Clark, C., Cortopassi, K.A., et al. (2011). Acoustic monitoring in terrestrial environments using microphone arrays: Applications, technological considerations and prospectus. *J. Appl. Ecol.* 48, 758–767.
34. Kays, R., Crofoot, M.C., Jetz, W., and Wikelski, M. (2015). ECOLOGY. Terrestrial animal tracking as an eye on life and planet. *Science* 348, aaa2478.
35. Hussey, N.E., Kessel, S.T., Aarestrup, K., Cooke, S.J., Cowley, P.D., Fisk, A.T., Harcourt, R.G., Holland, K.N., Iverson, S.J., Kocik, J.F., et al. (2015). ECOLOGY. Aquatic animal telemetry: A panoramic window into the underwater world. *Science* 348, 1255642.
36. Parks, S.E., Searby, A., Célérier, A., Johnson, M.P., Nowacek, D.P., and Tyack, P.L. (2011). Sound production behavior of individual North Atlantic right whales: Implications for passive acoustic monitoring. *Endanger. Species Res.* 15, 63–76.
37. Van Doren, B.M., and Horton, K.G. (2018). A continental system for forecasting bird migration. *Science* 361, 1115–1118.
38. Larkin, R.P., and Szafoni, R.E. (2008). Evidence for widely dispersed birds migrating together at night. *Integr. Comp. Biol.* 48, 40–49.
39. Chapman, J.W., Drake, V.A., and Reynolds, D.R. (2011). Recent insights from radar studies of insect flight. *Annu. Rev. Entomol.* 56, 337–356.
40. Guttal, V., and Couzin, I.D. (2010). Social interactions, information use, and the evolution of collective migration. *Proc. Natl. Acad. Sci. USA* 107, 16172–16177.
41. Buhl, J., Sumpter, D.J.T., Couzin, I.D., Hale, J.J., Despland, E., Miller, E.R., and Simpson, S.J. (2006). From disorder to order in marching locusts. *Science* 312, 1402–1406.
42. Berdahl, A., Torney, C.J., Ioannou, C.C., Faria, J.J., and Couzin, I.D. (2013). Emergent sensing of complex environments by mobile animal groups. *Science* 339, 574–576.
43. Santora, J.A., Sydeman, W.J., Schroeder, I.D., Wells, B.K., and Field, J.C. (2011). Mesoscale structure and oceanographic determinants of krill hotspots in the California Current: Implications for trophic transfer and conservation. *Prog. Oceanogr.* 91, 397–409.
44. Goldbogen, J.A., Cade, D.E., Wisniewska, D.M., Potvin, J., Segre, P.S., Savoca, M.S., Hazen, E.L., Czapanskiy, M.F., Kahane-Rapport, S.R., DeRuiter, S.L., et al. (2019). Why whales are big but not bigger: Physiological drivers and ecological limits in the age of ocean giants. *Science* 366, 1367–1372.
45. Goldbogen, J.A., Cade, D.E., Boersma, A.T., Calambokidis, J., Kahane-Rapport, S.R., Segre, P.S., Stimpert, A.K., and Friedlaender, A.S. (2017). Using Digital Tags With Integrated Video and Inertial Sensors to Study Moving Morphology and Associated Function in Large Aquatic Vertebrates. *Anat. Rec. (Hoboken)* 300, 1935–1941.
46. Goldbogen, J.A., Stimpert, A.K., DeRuiter, S.L., Calambokidis, J., Friedlaender, A.S., Schorr, G.S., Moretti, D.J., Tyack, P.L., and Southall, B.L. (2014). Using accelerometers to determine the calling behavior of tagged baleen whales. *J. Exp. Biol.* 217, 2449–2455.
47. Szesciorka, A.R., Calambokidis, J., and Harvey, J.T. (2016). Testing tag attachments to increase the attachment duration of archival tags on baleen whales. *Anim. Biotelem.* 4, 18.

48. Calambokidis, J., Fahlbusch, J.A., Szesciorka, A.R., Southall, B.L., Cade, D.E., Friedlaender, A.S., and Goldbogen, J.A. (2019). Differential Vulnerability to Ship Strikes Between Day and Night for Blue, Fin, and Humpback Whales Based on Dive and Movement Data From Medium Duration Archival Tags. *Front. Mar. Sci.* 6, 543.
49. Cline, D.E., and McGill, P.. pam-decimate-notebook, Available at. <https://bitbucket.org/mbari/pam-decimate-notebook/src/master/>.
50. Rivers, J.A. (1997). Blue whale, *Balaenoptera musculus*, vocalizations from the waters off central California. *Mar. Mamm. Sci.* 13, 186–195.
51. Leroy, E.C., Samaran, F., Bonnel, J., and Royer, J.Y. (2016). Seasonal and diel vocalization patterns of Antarctic blue whale (*Balaenoptera musculus intermedia*) in the Southern Indian Ocean: A multi-year and multi-site study. *PLoS ONE* 11, e0163587.
52. Haver, S.M., Rand, Z., Hatch, L.T., Lipski, D., Dziak, R.P., Gedamke, J., et al. (2020). Seasonal trends and primary contributors to the low-frequency soundscape of the Cordell Bank National Marine Sanctuary. *Journal of the Acoustical Society of America* 148 (2), 845–858.
53. Širović, A., Hildebrand, J.A., Wiggins, S.M., and Thiele, D. (2009). Blue and fin whale acoustic presence around Antarctica during 2003 and 2004. *Mar. Mamm. Sci.* 25, 125–136.
54. Koblick, D. (2020). Vectorized Solar Azimuth and Elevation Estimation (<https://www.mathworks.com/matlabcentral/fileexchange/23051-vectorized-solar-azimuth-and-elevation-estimation>). MATLAB Cent. File Exch.
55. 2018b). MATLAB (Natick, Massachusetts, United States: The MathWorks, Inc.).
56. R Core Team. (2019). R: A language and environment for statistical computing. Vienna, Austria. <http://www.R-project.org/>.
57. Collins, M.D. (1993). A split-step Pade solution for the parabolic equation method. *J. Acoust. Soc. Am.* 93, 1736–1742.
58. Cade, D.E., Friedlaender, A.S., Calambokidis, J., and Goldbogen, J.A. (2016). Kinematic Diversity in Rorqual Whale Feeding Mechanisms. *Curr. Biol.* 26, 2617–2624.
59. McDonald, M.A., Calambokidis, J., Teranishi, A.M., and Hildebrand, J.A. (2001). The acoustic calls of blue whales off California with gender data. *J. Acoust. Soc. Am.* 109, 1728–1735.
60. Stimpert, A.K., Lammers, M.O., Pack, A.A., and Au, W.W.L. (2020). Variations in received levels on a sound and movement tag on a singing humpback whale: Implications for caller identification. *J. Acoust. Soc. Am.* 147, 3684–3690.
61. Stimpert, A.K., DeRuiter, S.L., Falcone, E.A., Joseph, J., Douglas, A.B., Moretti, D.J., Friedlaender, A.S., Calambokidis, J., Gailey, G., Tyack, P.L., et al. (2015). Sound production and associated behavior of tagged fin whales (*Balaenoptera physalus*) in the Southern California Bight. *Anim. Biotelem.* 3, 23.
62. Saddler, M.R., Bocconcelli, A., Hickmott, L.S., Chiang, G., Landea-Briones, R., Bahamonde, P.A., Howes, G., Segre, P.S., and Sayigh, L.S. (2017). Characterizing Chilean blue whale vocalizations with DTAGs: a test of using tag accelerometers for caller identification. *J. Exp. Biol.* 220, 4119–4129.
63. Cade, D.E., Barr, K.R., Calambokidis, J., Friedlaender, A.S., and Goldbogen, J.A. (2018). Determining forward speed from accelerometer jiggle in aquatic environments. *J. Exp. Biol.* 221, jeb170449.
64. Jos. (2020). RUNMEAN. (<https://www.mathworks.com/matlabcentral/fileexchange/10113-runmean>), MATLAB Cent. File Exch.
65. Center for Conservation Bioacoustics. (2014). Raven Pro: Interactive Sound Analysis Software (Version 1.5). [Computer software]. Ithaca, NY: The Cornell Lab of Ornithology, Available from. <http://ravensoundsoftware.com/>.
66. Lewis, L.A., and Širović, A. (2018). Variability in blue whale acoustic behavior off southern California. *Mar. Mamm. Sci.* 34, 311–329.
67. Johnson, M.P., and Tyack, P.L. (2003). A digital acoustic recording tag for measuring the response of wild marine mammals to sound. *IEEE J. Oceanic Eng.* 28, 3–12.
68. Simon, M., Johnson, M., and Madsen, P.T.T. (2012). Keeping momentum with a mouthful of water: behavior and kinematics of humpback whale lunge feeding. *J. Exp. Biol.* 215, 3786–3798.

## STAR★METHODS

### KEY RESOURCES TABLE

REAGENT or RESOURCE	SOURCE	IDENTIFIER
Deposited Data		
Bio-logging, passive acoustics, and acoustic propagation model data	GitHub	<a href="https://github.com/woestreich/blue-whale-migration">https://github.com/woestreich/blue-whale-migration</a>
Software and Algorithms		
All code for data and statistical analysis	GitHub	<a href="https://github.com/woestreich/blue-whale-migration">https://github.com/woestreich/blue-whale-migration</a>
MATLAB 2018b	MathWorks	<a href="https://www.mathworks.com/downloads/">https://www.mathworks.com/downloads/</a>
R 3.6.1	The R Project for Statistical Computing	<a href="https://www.r-project.org/">https://www.r-project.org/</a>
RavenPro v1.5	The Cornell Lab of Ornithology Center for Conservation Bioacoustics	<a href="https://ravensoundsoftware.com/software/raven-pro/">https://ravensoundsoftware.com/software/raven-pro/</a>
Experimental Models: Organisms/Strains		
Blue whale, <i>Balaenoptera musculus</i>	Continental Shelf Edge, Northeast Pacific Ocean, California, USA	Taxonomy ID: 9711
Other		
Fastloc® GPS	Wildlife Computers	<a href="https://wildlifecomputers.com/data/technologies/fastloc/">https://wildlifecomputers.com/data/technologies/fastloc/</a>

### RESOURCE AVAILABILITY

#### Lead Contact

Further information and requests should be directed to and will be fulfilled by the Lead Contact, William Oestreich ([woestreich@stanford.edu](mailto:woestreich@stanford.edu)).

#### Materials Availability

This study did not generate new unique reagents

#### Data and Code Availability

All data and code used for analysis and visualization in this study are available via GitHub: <https://github.com/woestreich/blue-whale-migration>

### EXPERIMENTAL MODEL AND SUBJECT DETAILS

All tagging efforts and tag deployments on blue whales (*Balaenoptera musculus*) were conducted under authority of a scientific research permit under the Marine Mammal Protection Act and Endangered Species Act (NMFS Permits #16111 and 21678) and under Stanford University IACUC protocols.

### METHOD DETAILS

To study blue whale behavior across individual and regional population levels, we employed bio-logging and passive acoustic monitoring (PAM) methods, respectively. To quantify vocal behavior of the population at a regional scale, we used an acoustic index metric (blue whale B call index (CI); [Figure 1B](#)). While blue whales in the Northeast Pacific also produce non-song (type “D” calls), we focus exclusively on song-associated A and B calls in all acoustic analyses presented here. Daily CI was calculated over ~4.75 years (August 2015–April 2020) from nearly-continuous acoustic data collected via the Monterey Accelerated Research System (MARS) cabled observatory. To test the individual-level behavioral context of population scale patterns identified via PAM, we turn to whale-borne bio-logging approaches [[9, 45–48](#)].

#### Population-level behavior

All passive acoustic data for the analyses presented here were collected via Ocean Sonics icListen HF omnidirectional hydrophones [[15](#)] deployed sequentially and connected to the Monterey Accelerated Research System (MARS) cabled observatory on Smooth Ridge (36°42.75'N, 122°11.21'W; depth 891 m) on the continental slope outside Monterey Bay, CA. The first hydrophone had a

GeoSpectrum M24HF element and was deployed between 28 July 2015 and 13 June 2017. The second had a Reson TC4059-1 element and has been deployed since 13 June 2017. Frequency-dependent calibration data were provided by the manufacturer, yet only the lowest frequency sensitivity is relevant to the low-frequency calls of blue whales:  $-168.8$  dBV re  $\mu\text{Pa}$  at 26 Hz, and  $-177.8$  dBV re  $\mu\text{Pa}$  at 250 Hz, respectively. These hydrophones sampled at a rate of 256 kHz with bandwidth of 10 Hz to 200 kHz. Acoustic sampling from these instruments was nearly continuous over the study period, with 95% coverage during the  $\sim 4.75$ -year study period (5 full blue whale song seasons). All recordings were decimated to a sampling rate of 2 kHz before analysis [49].

The majority of acoustic research on this population has focused on the song-associated B call, largely due to its predictable spectral characteristics, long range detectability, and its status as the most common and highest received-level unit of the song-associated vocalizations [18, 19, 50]. However, significant overlap between abundant individual B calls can create a “chorusing” effect of nearly continuous energy in specific frequency bands, making detection of individual B calls impractical. This chorusing effect has previously been documented for both blue and fin whales [19, 51], and was present in the acoustic data collected in this study. As a result, we quantified intensity of blue whale song via calculation of energy-based “call index” values for blue whale B calls rather than via individual call detection. While call indices of this nature do not distinguish between many distant and few close callers (and therefore may have limited utility in some other contexts), CI is a useful tool for summarizing song intensity and is necessitated by the presence of chorusing.

Building upon acoustic power methods introduced by previous studies for fin [19, 52] and blue [53, 52] whales, the blue whale B call index (CI) was calculated as a signal to noise ratio between peak and background frequencies in calibrated long-term spectral averages (LTSAs). The frequency resolution of the LTSAs was 1 Hz, which enabled clear distinction of the energy peak of B calls (Figure 1B). The temporal resolution of the LTSAs was 1 min, which effectively quantified the energy of these relatively long-duration calls ( $\sim 10$  to 25 s), while allowing accurate assignment of each minute to solar elevation categories, as required to study diel variation (nautical definitions:  $< -12^\circ$  solar elevation for night;  $-12$  to  $0^\circ$  for dusk/dawn;  $> 0^\circ$  for day). Solar elevation for each minute was computed using the SolarAzEl function [54] for MATLAB (using version R2018b), with location specified as the ocean surface above the MARS hydrophone. Within each solar elevation bin and for each day, frequency dependent mean LTSA spectrum levels were averaged, then CI was calculated from each daily mean spectrum. CI peak values were calculated as the mean across 43–44 Hz (3<sup>rd</sup> harmonic, strongest harmonic of the B call); background values were calculated as the mean of values at 37 and 50 Hz (frequencies proximate to the peak frequencies but situated between other biological signals; Figure 1B). Daily CI results were then aggregated by month across the  $\sim 4.75$ -year acoustic time-series, and presented as a statistical summary with percentiles (10<sup>th</sup>, 25<sup>th</sup>, 50<sup>th</sup>, 75<sup>th</sup>, 90<sup>th</sup>) and mean (Figure 2B). Monthly aggregations of daily resolution data allowed for understanding of both central tendency and spread in monthly CI. Diel patterns in CI were calculated as a ratio,  $\text{CI}_{\text{night}}:\text{CI}_{\text{day}}$ , again at daily resolution and aggregated by month for statistical summary (Figure 2C). Because CI itself is a ratio, with a value of 1 indicating song signal undetectable above background noise, computing  $\text{CI}_{\text{night}}:\text{CI}_{\text{day}}$  first required subtraction of the minimum of all monthly values, including both  $\text{CI}_{\text{night}}$  and  $\text{CI}_{\text{day}}$ , in order to properly scale  $\text{CI}_{\text{night}}:\text{CI}_{\text{day}}$  to the range of variation. All calculations for CI and  $\text{CI}_{\text{night}}:\text{CI}_{\text{day}}$  were performed via custom software written for MATLAB 2018b [55] (see Data and Code availability for details). For both CI and  $\text{CI}_{\text{night}}:\text{CI}_{\text{day}}$  tests of significant month-to-month changes in mean were conducted via two-sided t tests of daily values from subsequent months in R version 3.6.1 [56].

In order to characterize the sampling domain of the MARS hydrophone for blue whale B call detection, acoustic transmission loss was modeled at 44 Hz (3<sup>rd</sup> harmonic of the blue whale B call) using a wave-theory parabolic equation model that accounts for absorption in both the water column and the bottom, scattering in the water column and at the surface and bottom, geometric spreading (spherical and cylindrical), refraction, and diffraction [57]. Specification of regional ocean temperature and salinity was based on the November climatology from the US Navy Generalized Digital Environmental Model (GDEM). Bathymetry was specified at 250 m resolution. The source level of 171 dB re  $1 \mu\text{Pa}\cdot\text{m}$  was based on published *in situ* measurements ( $\sim 175$  dB re  $1 \mu\text{Pa}^2/\text{Hz}$  @ 1 m minus 4 dB for conversion to tonal spectral level [22]) and used to compute received levels at MARS to characterize the spatial domain around the hydrophone over which B calls should be detectable under median noise conditions (Figure 2A). Sound source depth was specified as 14.83 m, the mean B call depth from tag deployments in this analysis.

### Individual-level behavior

To investigate individual-level behavior, blue whales (*B. musculus*) were tagged from 2017–2019 along the shelf break of central and northern California, USA. Individual whales were approached using a 6 m rigid hull inflatable boat and tagged using a 6 m pole with one of two different tag types: (1) short duration, high frequency ( $\sim 2$ –36 h deployment) suction cup-attached video and 3D accelerometer tags [45, 58] manufactured by Customized Animal Tracking Solutions (CATS); and (2) medium duration, medium frequency ( $\sim 2$ –32 day deployment) dart-attached 3D accelerometer tags [47, 48] manufactured by Wildlife Computers, Inc. CATS tag accelerometers sampled at 400 Hz and were analyzed at full resolution for call detection (see below). CATS tag magnetometer and gyroscopes sampled at 50 Hz, and pressure, light, temperature, and integrated Fastloc® GPS sampled at 10 Hz. All movement data were downsampled to 10 Hz before further processing. TDR10 tag accelerometers sampled at 32 Hz, and were similarly analyzed at full resolution for call detection. All tag-derived data used in this study were collected under NMFS permits 16111 and 21678.

To quantify song call rates of individual tagged animals, we built upon the accelerometer-based call detection methods introduced by Goldbogen et al. [46]. As with some other baleen whales, the high source level of blue whale vocalizations [22, 59] and the potential proximity of conspecifics make determination of the individual producing vocalizations detected by tag-mounted hydrophones

difficult [60]. Tag-mounted accelerometers detecting vibrations at the fundamental and harmonic frequencies of animal vocalizations have been proposed [46] and utilized [61] to identify the calls produced by tagged fin whales (*Balaenoptera physalus*). These accelerometer-detected calls can then be placed in behavioral context via synchronization with other tag-mounted sensors [61]. While the potential for missed call detections or non-tagged-animal call detections with this method has been discussed and tested for other vocalization (blue whale D call) and tag types (DTAG) [62], previous successes with this method [46, 60, 61] as well as a lack of acoustic or focal follow data for medium-duration TDR10 tag deployments make this accelerometer method the only method available for detecting possible tagged-animal vocalizations and contextualizing this vocal behavior. Simultaneous deployment of CATS tags on proximate pairs of foraging blue whales in the present study resulted in accelerometer-based detection of vocalizations on only one tag, but hydrophone-based detections on both, further supporting this method of identifying the calling individual. We applied this method of identifying calls produced by tagged individuals to both short duration, high frequency (400 Hz; CATS tags) and medium duration, medium frequency (32 Hz; TDR10 tags) tag-mounted accelerometers (Figure S2). While the highest amplitude harmonics of blue whale A (5<sup>th</sup> harmonic; ~80 Hz) and B (3<sup>rd</sup> harmonic, ~44 Hz) calls typical in acoustic detection are above the Nyquist frequency of the TDR10 accelerometers, the fundamental frequency (~15 Hz for A and B calls) displays the highest amplitude signal in accelerometer-based detection for both CATS [63] and TDR10 (Figure S2) tags. This allows for detection of both A and B calls in the 32 Hz TDR10 accelerometer signal. The ability to detect clear song sequences in the TDR10 accelerometer signal spaced between surface breaths in the manner described in previous individual-scale studies [9] (e.g., Figure S2), even when paired individuals were known to be present in close proximity (e.g., deployment Bm190916-TDR14; Figure 4B) further bolsters confidence in extension of this method to TDR10 tags. As such, only deployments ( $n = 2$ ) with these clearly identifiable song sequences were analyzed in the present study.

For both CATS and TDR10 deployments, triaxial tag accelerometry data were first low-pass filtered (running mean with window size of  $2f + 1$ , where  $f$  is the accelerometer sampling frequency) [64]. For each deployment, filtered data were then converted to a spectrogram visualization (Fast Fourier Transform with 1024 sample window size, 95% overlap, and Hann window) for manual call detection (Figure S2). Manual call detections audits were completed in RavenPro v1.5 [65]. Of fifty-two CATS tag deployments on *B. musculus* from 2017–2019, song-associated vocalizations (A, B, and C calls) were detected in thirteen deployments (Table S1). For TDR10 deployments on *B. musculus* from 2017–2019, two of fourteen deployments yielded consistently identifiable song-associated vocalizations. Only A and B call detections were included in tag-based call analyses, as C calls (1) were not often clearly detectable in the TDR10 accelerometer signal and (2) are not generally well-understood in terms of how often blue whale songs contain C calls. While a previous study [66] has described nuanced differences between single A or B calls, paired A and B calls, and repetitive “ABB” phrases, we aggregated song calls (A + B) in our analysis for two reasons: (1) for the sake of comparability to population-scale song production; and (2) because we found similar results when including both A and B and only B calls, suggesting that these more nuanced patterns in song call patterns did not have a significant effect on the diel patterns described here from years of data. Similar to B call index values, all detected A and B calls were binned into solar elevation categories using the nautical definition for dawn and dusk and the SolarAzEl function [54] for MATLAB.

Tag accelerometer, magnetometer, gyroscope, pressure, light, and temperature data were downsampled to 10 Hz (CATS) and 8 Hz (TDR-10), and animal orientation was calculated (with correction for tag orientation on the animal) using custom-written scripts in MATLAB (following [58, 67]). Animal speed for all deployments was determined using the amplitude of tag vibrations [63]. Lunge feeding on krill is highly stereotypical and individual lunges can be identified from the tag records as peaks in speed followed by rapid deceleration that corresponds to increases in dynamic body acceleration as well as changes in pitch, roll and heading associated with maneuvering [58, 68]. All lunge detections on both CATS and TDR10 deployments were performed manually using these stereotypical signatures of rorqual lunge feeding.

For each the two TDR10 deployments analyzed in the present study (Figure 4), mean and standard error of daily lunge and song call rates during night and day  $h$  were calculated and reported. Two-way t tests were conducted in R Version 3.6.1 [56] to compare the mean values of daily night-minus-day song call production rates during foraging and migration behavioral states.

## QUANTIFICATION AND STATISTICAL ANALYSIS

Statistical analysis and quantification for this study was conducted in R Version 3.6.1 [56] and MATLAB 2018b [55]. All acoustic data analyses described above (Methods Details, Population-level behavior) were conducted in MATLAB. All tag data analyses (Methods Details, Individual-level behavior) were also conducted in MATLAB. Descriptive statistics (percentiles, means, and medians reported throughout the Main Text and STAR Methods) were calculated in MATLAB. All statistical tests of significance (two-way t tests (equal variance of distributions not assumed) for difference in means between sequential months of aggregated daily acoustic data (Figure 2); two-way t tests (equal variance of distributions not assumed) for difference in means between daily night-minus-day song call production pre- and post-behavioral transition on medium-duration tags (Figure 4)) were conducted in R. Statistical significance for all aforementioned t tests was defined as  $p < 0.05$ . Code used to complete all calculations and statistical analyses in MATLAB and R is available via GitHub (see Data and Code Availability). Sample sizes ( $n$ ) vary by context throughout this study, and are reported with units (e.g.,  $n = 15$  tag deployments) throughout the Main Text and STAR Methods.

**Current Biology, Volume 30**

**Supplemental Information**

**Animal-Borne Metrics Enable Acoustic**

**Detection of Blue Whale Migration**

**William K. Oestreich, James A. Fahlbusch, David E. Cade, John Calambokidis, Tetyana Margolina, John Joseph, Ari S. Friedlaender, Megan F. McKenna, Alison K. Stimpert, Brandon L. Southall, Jeremy A. Goldbogen, and John P. Ryan**

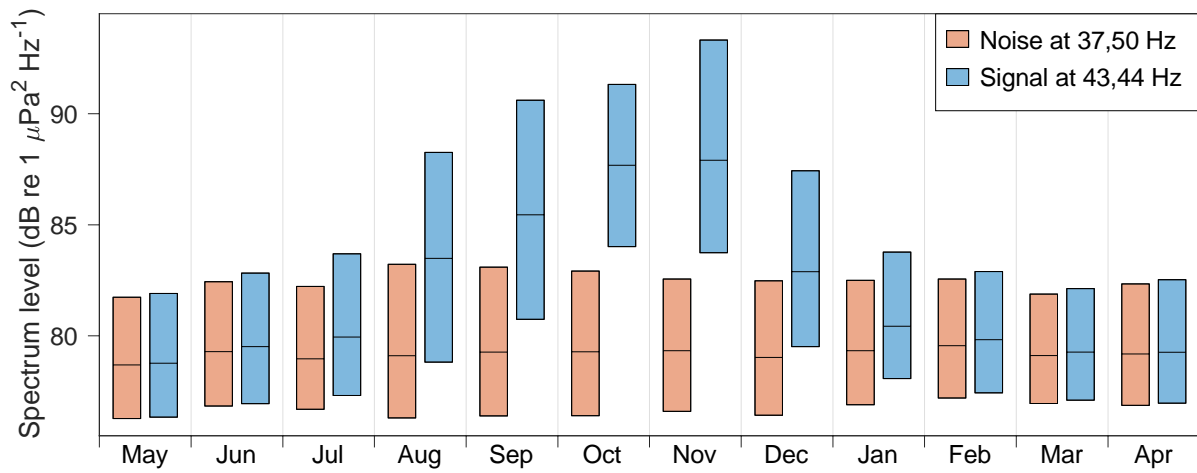


**Figure S1. Signal (blue whale B call 3<sup>rd</sup> harmonic) and noise (nearby background frequencies) statistics for call index (CI) calculation, Related to Figures 1B and 2A.** Boxes show 25<sup>th</sup> 50<sup>th</sup> and 75<sup>th</sup> percentiles of daily values across the five study years, colored by noise (red) and signal (blue), While noise bands in the CI calculation are relatively constant throughout the year, signal bands vary seasonally, indicating that the seasonal patterns described in Figure 2 are driven by blue whale song signal rather than variation in background noise conditions.

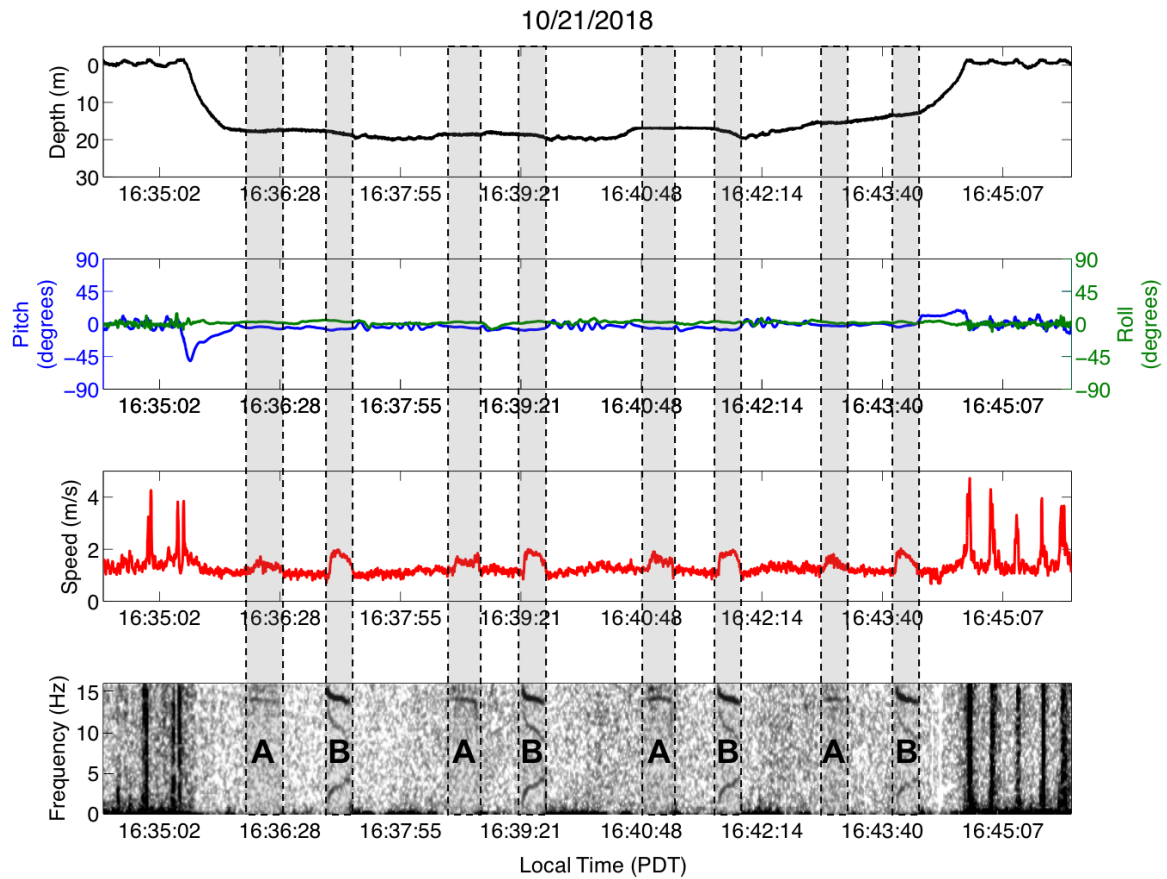


**Figure S2. Call detection from medium-duration TDR10 accelerometer data, Related to STAR Methods.** Panels display (top-to-bottom) time-synced depth, pitch and roll, speed, and low-pass-filtered Fast Fourier Transform of accelerometer signal (x-axis). Blue whale A and B calls are clearly identifiable in the accelerometry, seen as spectrogram features at the fundamental frequencies ( $\sim 15$  Hz) of blue whale A and B calls. These vocalizations are also visible as artifacts in the accelerometer jiggle-calculated speed profile.

<b>Year</b>	<b>CATS Deployments</b>	<b>TDR10 Deployments</b>	<b>Total Deployments</b>	<b>Total Hours</b>	<b>Total Calls (A + B)</b>	<b>Total Lunges</b>
<b>2017</b>	4	0	4	77.65	411	1107
<b>2018</b>	6	1	7	383.93	2549	2543
<b>2019</b>	3	1	4	202.55	1008	1242
<b>Total</b>	<b>13</b>	<b>2</b>	<b>15</b>	<b>664.13</b>	<b>3968</b>	<b>4892</b>

**Table S1. Summary of tag deployments with call and feeding lunge detections, Related to Figures 3 and 4.**